

MAPPING PERFORMANCE-TARGETED RETROFITTING TO SEISMIC FRAGILITY REDUCTION

Karim Aljawhari¹, Roberto Gentile², and Carmine Galasso^{1,2}

¹ Scuola Universitaria Superiore IUSS Pavia
Piazza della Vittoria, 15, 27100 Pavia, Italy
e-mail: karim.aljawhari@iusspavia.it

² University College London
Gower St, London WC1E 6BT, United Kingdom
e-mail: {r.gentile,c.galasso}@ucl.ac.uk

Abstract

This study investigates the improvement in the seismic performance of an archetype reinforced concrete (RC) frame due to varying structural retrofit levels. Specifically, the study attempts to map the increase of the displacement-based global ratio between capacity and life-safety demand (CDR_{LS}) to the reduction of seismic fragility. Such a reduction is characterized by the shift of the median fragility for different structure-specific damage states (DSs). The considered structure does not conform to modern seismic design requirements, and it is retrofitted using various techniques. Advanced nonlinear models are developed for the archetype frame, accounting for potential failure mechanisms, including flexural, joint, and shear failure. Three common retrofitting techniques are investigated, namely RC jacketing, steel jacketing, and fiber-reinforced polymers (FRP) wrapping of columns and joints. Each technique is specifically designed and proportioned to achieve predefined performance objectives (i.e., performance-targeted retrofitting), thus generating many retrofit alternatives. The improvement in seismic performance for the retrofitted frames is first characterized by computing the global CDR_{LS} , which can be obtained using nonlinear pushover analysis combined with the Capacity Spectrum Method. Subsequently, cloud-based nonlinear time-history analyses are performed to derive fragility relationships for the as-built and retrofitted configurations, monitoring the variation in the median fragility for all DSs. Finally, the global CDR_{LS} increase due to retrofitting is correlated with the corresponding shift in the median fragility. A linear trend is found, and it is used accordingly to develop simple models that engineers can implement to provide reasonable estimates for such shift once the global CDR_{LS} is known.

Keywords: Retrofitting strategies, fragility relationships, nonlinear analysis, reinforced-concrete frames, performance-based assessment.

1 INTRODUCTION

Many existing reinforced concrete (RC) buildings in earthquake-prone regions do not conform to modern seismic codes as they were mainly designed to resist gravity loads only. These buildings are vulnerable to severe damage or even collapse under moderate-to-high ground-shaking intensity levels [1]. This has led to significant economic and life losses, as demonstrated by numerous past earthquakes (*e.g.* [2], [3]).

To mitigate the consequences of earthquake events on such buildings and improve their seismic performance, structural retrofitting is often necessary. Such an approach has become very popular lately due to the ease of construction and cost-effectiveness compared to other drastic solutions like demolition and complete replacement.

Generally, retrofitting strategies aim to modify key structural parameters such as strength, ductility, and stiffness or reduce seismic demand. Several techniques (systems) are widely used to implement one or more strategies. For instance, adding RC shear walls (*e.g.* [4], [5]) or bracing (*e.g.* [6], [7]) to existing buildings improves both stiffness and lateral strength significantly. On the other hand, base isolation can be implemented to reduce seismic demands by simply decoupling the horizontal motion of the structure and that of the ground [8].

Many challenges may arise in adopting the above techniques, which are related to the architectural compatibility of the intervention, its invasiveness, the need to modify existing foundations or adding new ones, in addition to the high implementation costs and long duration of the work. Therefore, less-invasive retrofitting techniques, which represent the main focus of the current study, are more common and popular. Examples include wrapping structural elements with fiber-reinforced polymers (FRP), and jacketing columns using either RC or steel jackets. These local techniques are fundamentally less expensive, and they pose a minimal degree of invasiveness/business interruption compared to RC shear walls or bracing.

Most of the past research focused on the experimental investigation of different retrofitting techniques and developing analytical and numerical models to simulate their effect on existing structural elements and/or systems. For instance, some studies investigated the effects of steel jackets on RC columns experimentally and developed design procedures (*e.g.* [9]–[12]), while others explored FRP retrofitting (*e.g.* [12]–[15]) and RC jacketing for columns (*e.g.* [16], [17]).

Retrofitted buildings are expected to perform better against earthquake-induced ground shaking. However, field observations for those buildings under actual seismic events are still scarce, indicating the lack of sufficient empirical fragility and vulnerability models in the literature. This demonstrates the need for numerically developing such models considering different retrofitting techniques and geometric layouts, which are essential for applications related to seismic risk reduction and increasing resilience of earthquake-prone communities around the world. This has indeed attracted many research efforts in the past few decades, but a limited number of studies is available. A detailed review of such studies is outside of the current paper's scope, but a few are briefly discussed to provide the reader with some background.

Some studies developed fragility relationships considering FRP, RC jacketing, base isolation, and adding shear walls (*e.g.* [18], [19]). However, the fragility models accounted for collapse only, without considering other damage states (DSs). Moreover, retrofitting was either applied based on engineering judgment, *i.e.* without properly accounting for structure-specific seismic deficiencies or predefined performance objectives [18], or considering only one, rather than multiple, performance objectives (*e.g.* [19], [20]). Other studies considered applying different retrofitting techniques with varying intervention levels to achieve different performance objectives (*e.g.* [21], [22]), but only collapse fragility relationships were evaluated.

The current study investigates the improvement in seismic performance of an archetype RC frame located in a high-seismicity zone considering varying levels of retrofitting intervention

using three different techniques: FRP wrapping, steel jacketing, and RC jacketing. Each one is designed to achieve multiple predefined performance objectives, resulting in many realizations of retrofitted buildings. These cases are first assessed by quantifying the displacement-based global ratio between capacity and life-safety (LS) demand (CDR_{LS}), or simply capacity-to-demand ratio. This parameter is equivalent to the “Percentage of New Building Standard” introduced first by [23]. Subsequently, fragility relationships are developed accounting for different structure-specific DSs to investigate the effects of retrofitting on building-level fragility. An attempt is also made to correlate the CDR_{LS} to the shift of fragility relationships due to retrofitting to derive a simplified model that can be used to estimate the shift in fragility based on the CDR_{LS} value. A generalization of such a simplified model might be used, among various possible usages, to analyze and/or design scenario-based retrofit implementation plans at a portfolio level by implementing it in a regional seismic risk model. Although such generalization is out of scope herein, it is deemed worthy of investigation.

The paper is organized as follows. Section 2 introduces the methodology implemented in the current study. This includes a description of the geometry and properties/details of the case-study structure, an introduction to the adopted retrofitting techniques, the nonlinear modeling strategies for both the as-built and retrofitted case studies, the definition of DSs, and ground-motion selection. Section 3 presents the design of the retrofitted case studies, the initial performance assessment for both as-built and retrofitted cases, followed by fragility analysis. Section 4 addresses the proposed mapping between the capacity-to-demand ratio to seismic fragility median. Finally, section 5 provides some concluding remarks, highlighting the limitation of the study and future steps.

2 METHODOLOGY

2.1 Case-study building

An older five-storey, four-bay RC moment-resisting frame with a total height of 15 m and a uniform bay width of 4.5 m is considered, as shown in Figure 1. This frame is designed to resist gravity loads only according to the Royal Decree n. 2229 in Italy in 1939, which regulated the design of RC frames until 1974. Following this decree, simulated design is performed to define the proportioning and detailing of all the structural elements, using allowable stress design.

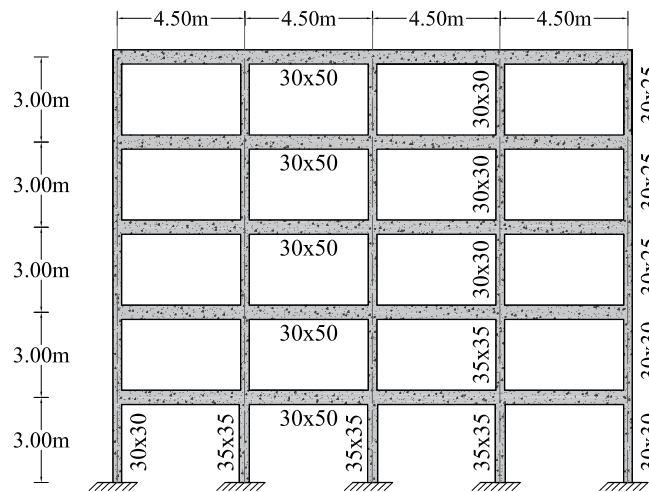


Figure 1: Elevation view of the 5-storey case-study frame (cross-sectional dimensions are in cm)

This frame does not satisfy the main seismic design provisions such as those for capacity design and strong-column-weak-beam. Beams and columns are poorly confined, and the latter elements have a very low amount of longitudinal reinforcement (*i.e.* less than 1%). Moreover, the joints lack transverse reinforcement, use smooth bars, and improper anchorage [24]–[26]. This makes the frame susceptible to developing brittle failure mechanisms such as joint failure, soft-storey, and shear failure. Typical average values for the material properties are used, which are representative of that era. Specifically, the average compressive strength of the concrete (f_{cm}) is 16.5 MPa, in compliance with other studies (*e.g.* [27], [28]). The average yield strength (f_{ym}) of reinforcing steel is 330 MPa [29]–[31].

2.2 Selected retrofitting techniques

Three different retrofitting techniques are investigated in this study: FRP wrapping, steel jacketing, and RC jacketing. Typical cross-sections for columns retrofitted using these techniques are illustrated in Figure 2.

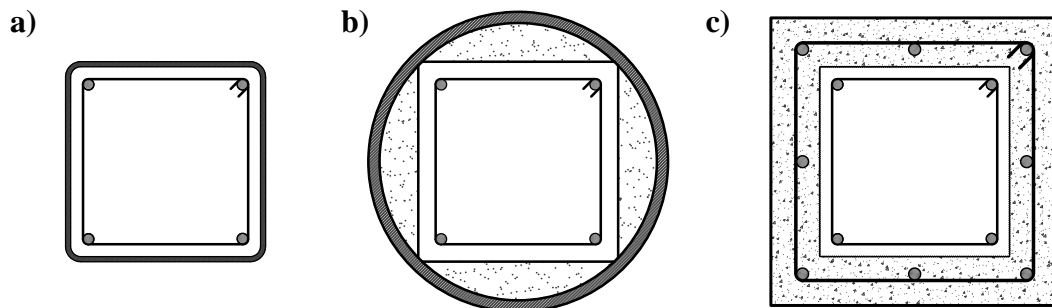


Figure 2: Typical cross-sections of a column retrofitted using (a) FRP; (b) steel jacketing; and (c) RC jacketing

FRP wrapping is mainly used for joints and columns to prevent brittle shear failure mechanisms. It also provides a high level of confinement for columns, thus improving their ductility under extreme loading conditions (*e.g.* [13], [14]). The contribution of FRP wrapping to the stiffness and flexural strength is minimal as the unidirectional fibers are placed perpendicular to the longitudinal axis of columns.

Rectangular and elliptical steel jackets are another popular option to prevent shear failure of columns. They are also able to increase lateral stiffness due to the isotropic properties of steel [12]. However, only elliptical (or circular) steel jackets are used in the current study because they are very effective in improving confinement and ductility due to the continuous confining pressure they provide [9]. This technique also offers some enhancement of flexural strength. Conversely, experiments demonstrated that rectangular steel jackets lose much of their confinement efficiency (*e.g.* [9], [16]). A gap of 50 mm is deliberately left between the edges of the steel jacket and foundations/beams to prevent excessive flexural strength enhancement, which transfers forces to adjacent members [9].

RC jacketing is the most traditional and common technique in practice as it is characterized by a low cost and does not require specialized labor. It comprises encasing existing columns with a cast-in-place RC jacket to improve confinement, ductility, and both shear and flexural strengths. Continuous column jacketing in two consecutive floors also enhances joint behavior. The thickness of an RC jacket is controlled by the size of longitudinal and transverse reinforcement to be used, in addition to the minimum cover requirement (*e.g.* [16], [32]). Compared to the other two techniques, RC jacketing poses the highest level of invasiveness. It can notably increase the size of existing columns and might require extending reinforcement through slabs, foundations, and joints.

2.3 Design of retrofitting techniques

A trial-and-error design procedure is adopted for the three retrofitting techniques, aiming to achieve a predefined set of performance objectives, as explained later. For each technique, design iterations might vary with respect to detailing, geometric characteristics, and the number of retrofitted elements to ensure incremental improvements in seismic performance.

For the FRP technique, laminated pre-cured sheets with high-strength carbon fibers (CFRP) are wrapped around the full height of existing columns. The elasticity modulus (E_f) is equal to 140 GPa, ultimate tensile strength (F_{fu}) is 2000 MPa, and rupture strain (ϵ_{fu}) is 1.2% [33], assuming that each layer has a thickness of 0.5 mm. It is considered that the maximum number of FRP layers is five to ensure confinement efficiency [34]. It should be noted that the FRP is also used for joint retrofit in cases where joint failure is observed (mainly external ones).

On the other hand, full-height elliptical/circular steel jackets are used. The space between the steel jacket and retrofitted column can be filled with either grout material or plain concrete [9], [12]. The jackets are made of structural steel grade S235 with an average yield strength (f_{yj}) of 235 MPa and a minimum thickness of 1.5 mm, which is increased during the iterative design process. As mentioned earlier, a gap of 50 mm is left between the edges of steel jackets and column ends to prevent transferring forces to adjacent members [9].

In the case of RC jacketing, a full-height encasement of existing columns is made using cast-in-situ concrete, with the possibility of extending longitudinal reinforcement through foundations and slabs. RC jackets with a minimum thickness of 50 mm are adopted, with at least $4\Phi 14$ mm for external columns and $4\Phi 16$ mm for internal ones (Φ refers to the diameter). Hoops with $\Phi 8$ mm are used with a spacing not exceeding 150 mm. The reinforcement and/or jacket thickness are increased gradually during the iterative design, as stated earlier. The concrete material is characterized by f_{cm} of 33 MPa, while f_{ym} for the reinforcement is equal to 490 MPa.

2.4 Nonlinear modeling strategies

The nonlinear response of the case-study building is simulated by developing 2D numerical models using OpenSees [35]. Structural components are modeled as beam-column elements with finite-length plastic hinges to simulate the nonlinear flexural response, which is defined by performing moment-curvature analysis following the rules defined by [36] and [37]. The post-capping degrading response for the moment-curvature and the hysteretic parameters are assigned according to [38]. Additional shear springs are added in series to the beam-column element to account for potential shear failure modes, as illustrated in Figure 3. The backbone curve parameters for the shear response are calculated in accordance with [39]–[41].

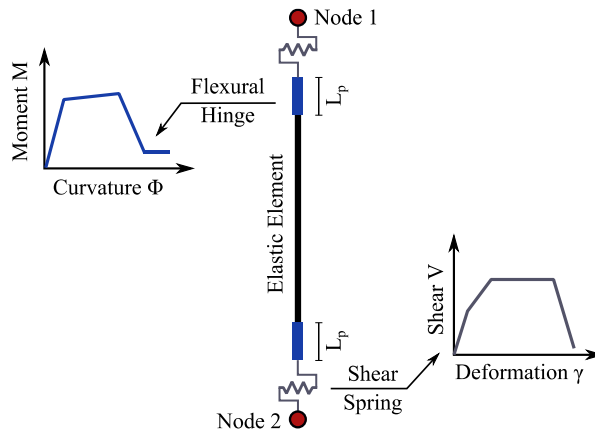


Figure 3: Modelling strategy for structural components

As mentioned earlier, joints in older Italian RC frames are characterized by the lack of transverse reinforcement and the use of smooth bars with end-hooks, particularly in external joints [24]–[26]. Therefore, the early failure of such joints leads the building to develop a brittle failure mechanism. Therefore, an additional spring is added in each beam-column joint zone. The parameters of the nonlinear material of joints are defined according to [38], which is a mechanics-based approach introduced in many other studies (*e.g.* [42], [43]).

To account for the effects of FRP on columns, the moment-curvature relationship is modified considering the confinement provided by this technique. This is achieved by first assuming that the entire column cross-section is confined rather than the core only since the FRP layers are wrapped around the external perimeter of the column. Next, the confinement pressure (f_l) due to FRP wrapping is calculated based on [13] and then the compressive strength and ultimate strain of the confined concrete (f_{cc} and ϵ_{ccu}) can be estimated based on [44] and [13], respectively. It should be noted that FRP wrapping around rectangular columns is less effective than circular ones because only inward corner forces provide the confinement in the former case instead of continuous pressure around the perimeter. Thus, a confinement effectiveness factor is used to reduce the value of f_l as per [33]. Moreover, the additional shear strength due to FRP is calculated and added to the shear strength of the as-built column in accordance with [13].

It should be noted that the unique failure modes pertaining to FRP, such as debonding and fracture mechanisms, are not explicitly modeled, assuming the FRP retrofitting is designed and installed appropriately so that the concrete and reinforcement will govern the softening behavior of the retrofitted elements at high levels of deformation (*e.g.* [22], [45]).

Steel jacketing is treated in a similar manner to FRP. The value of f_l is estimated as per [9], whilst f_{cc} and ϵ_{ccu} are found based on [44] and [16], respectively. These new values are adopted to modify the moment-curvature relationship. The additional shear strength due to the steel jacket is estimated according to [9].

Finally, columns retrofitted with RC jackets are treated as equivalent monolithic members. This assumption is deemed valid as long as the jackets are well constructed and the surface of existing columns is adequately treated (*e.g.* [45], [46]). However, to address the possibility of a poor bond between the new RC jackets and existing columns, it is recommended to use the as-built value of f_c for the entire cross-section and to assume that lateral confinement is provided solely by the hoops of the new RC jacket [16].

2.5 Damage state definition and thresholds mapping

Three structure-specific DSs are adopted in order to characterize different damage conditions, which reflect the performance level (PL) of the building. Each DS occurs when the structure attains a specific threshold defined with respect to an engineering demand parameter (EDP). This study adopts the maximum interstorey drift ratio (MIDR) as an EDP, which is a reliable and widely-used proxy to quantify global structural and nonstructural damage (at least in the case of drift-sensitive nonstructural components).

The MIDR thresholds are calibrated by assessing multiple measurable criteria during nonlinear static (*i.e.* pushover) analysis using a modal-pattern incremental load. These criteria are adopted from [47] and are also summarized in Table 1. The parameters θ_y and θ_u in Table 1 represent the yield and ultimate chord rotations, respectively. The latter parameter is evaluated according to [48]. It should be noted that the MIDR threshold for each DS is based on the first occurrence of any criterion among those shown in Table 1 (*e.g.* [47]).

The three DSs are described as follows: DS1, which accounts for moderate damage levels, is characterized by moderate structural and nonstructural damages with no significant yielding. The building here maintains the limited occupancy PL, but minor repairs may be required. DS2,

which corresponds to significant damage (SD), incorporates severe damages in both structural and nonstructural components, but buildings still retain some residual strength and stiffness. The building in DS2 meets the PL of life safety (LS), in which significant repairs are needed, which might not always be feasible. Finally, DS3 represents here the collapse-prevention PL, characterized by the full exploitation of strength and ductility. Minimal residual strength and stiffness remain in DS3, and the building is in a near-collapse condition [49].

Level/DS	DS1	DS2	DS3
Section Level	Reaching yield bending in a supporting column	Max. bending strength of a column is reached	Reaching shear failure in any element
Component Level	Reaching θ_y in any supporting column	Reaching 75% of the θ_u in any component	Reaching the θ_u in any component
Global Level	Reaching the global yield point of the structure	Reaching the maximum strength	About 20% drop in the maximum strength
General description	Moderate structural and nonstructural damage. No significant yielding of members	Severe structural and nonstructural damage. Some residual strength and stiffness retained	Full exploitation of strength and ductility. Low residual strength and stiffness

Table 1: Criteria used for mapping of DSs; adopted from [47]

The analytical formulation for θ_u requires inputting the amount of transverse reinforcement. This is directly applicable for the existing structural components and those retrofitted using RC jackets. In the case of FRP or steel jacketing, the concept of equivalent transverse reinforcement is implemented (*e.g.* [12], [22], [45]). In this approach, the FRP or steel jacketing can be simply converted to standard transverse reinforcement that mimics their effect by generating a lateral confining pressure equal to that produced by either of them.

2.6 Performance-targeted retrofitting

As indicated earlier, varying retrofitting levels are designed and applied to the case-study structure to meet some predefined performance objectives (*i.e.* performance-targeted retrofitting). These objectives represent achieving specific PLs (or DSs), either fully or partially, under a selected level of seismic hazard (*e.g.* [50]). The selected hazard level in all performance objectives is the one associated with life safety, *i.e.* corresponding to a mean return period of 475 years (*e.g.* [48], [50], [51]), as it is the most relevant and widely-used hazard level for the design and assessment of buildings – and for which hazard maps/curves are readily available.

To investigate whether a retrofitting intervention achieves a particular performance objective, the displacement-based global ratio between capacity and LS seismic demand, *i.e.* CDR_{LS} is considered. The LS displacement demand is calculated by transforming the force-deformation relationship (*i.e.* capacity curve) derived from pushover analysis to a capacity spectrum of an equivalent single-degree-of-freedom (SDoF) system plotted in the acceleration-displacement response spectra (ADRS) space. Subsequently, the capacity spectrum method (CSM) is applied in order to obtain a graphical representation of the performance [52]. A summary of the selected performance objectives is provided in Table 2.

It should be highlighted that the seismic demand used to design and assess different retrofitting cases is characterized by a Type 1 response spectrum according to [53], with a peak ground acceleration (PGA) of 0.30g and ground type C to account for high-seismicity conditions.

Performance objective	Description
No-collapse performance	Achieve the collapse-prevention PL (DS3) against the LS seismic demand
Limited performance	Partially achieve significant damage PL (DS2) against LS demand ($CDR_{LS} \approx 75\%$)
Basic performance	Achieve the significant-damage PL (DS2) against LS demand (100% of CDR_{LS})
Advanced performance	Achieve moderate damage (DS1; limited occupancy) against LS seismic demand

Table 2: Selected performance objectives for seismic retrofitting

2.7 Fragility relationships and selection of ground-motion records

Retrofitting of structures can result in a significant improvement in their seismic fragility. Fragility relationships characterize the conditional probability of exceeding different building-level, structure-specific DSs given a ground-shaking intensity level (IM), *i.e.* $P(DS \geq dsi|IM)$. It is possible to derive fragility relationships by performing nonlinear time-history analysis (NLTHA) using a set of unscaled (as-recorded) ground-motion records, *i.e.* by performing cloud analysis [54], among other alternative approaches. Hence, clouds of IM vs. EDP are developed and appropriate probabilistic seismic demand models (PSDMs) are fitted via power-law regression, which allows deriving fragility relationships using a closed-form solution [55] as shown in Eq. (1)-(2).

$$EDP = aIM^b \quad (1)$$

$$P(DS \geq dsi|IM) = \Phi\left(\frac{\ln(IM/\mu)}{\beta}\right) \quad (2)$$

where a and b are the regression parameters, μ is the median IM, and β is the dispersion. The records used for the NLTHA are adopted from the SIMBAD (Selected Input Motions for displacement-Based Assessment and Design) database developed by [56], which incorporates 467 three-component records related to shallow crustal earthquakes with magnitudes between 5.0 and 7.3 and epicentral distances less than 30 km [56]. To reduce the computational effort yet maintaining the engineering significance of the analysis, only 150 records are selected following the same criteria defined in [20], [57]. Specifically, the ground motions are ranked with respect to their PGA, obtained as the geometric mean of the two horizontal components. For each ground motion, the horizontal component with the highest PGA is kept, and then the 150 records with the highest ranking are selected. Such procedure is compatible with cloud analysis, and therefore it does not require a site-specific record selection. Moreover, this approach is deemed appropriate for regional-scale seismic risk assessment of building portfolios, especially when coupled with optimal IMs.

The IM implemented in this study is the geometric mean of the 5%-damped spectral acceleration over a specific range of vibration periods (avgSa). Such an IM accounts indirectly for the effects of higher modes, in addition to the period elongation due to the strength and stiffness degradation as well as the damage of different components (*e.g.* [58]–[60]). This IM, compared to other conventional ones like the spectral acceleration at the fundamental period $Sa(T_1)$, minimizes response variability, and it has a higher relative sufficiency [61].

The avgSa in this study is calculated considering 10 equally-spaced periods ranging within $0.2T_1$ and $1.5T_1$ (e.g. [62]). However, to allow for fragility comparison between the as-built and the retrofitted case-studies, the same period range is adopted for all of them, which is based on T_1 of the as-built case. This assumption is deemed appropriate as the change in T_1 for the majority of retrofitted cases is not very significant.

3 RESULTS AND DISCUSSION

3.1 Initial assessment for the as-built structure

To understand the response and failure mechanism of the as-built case-study structure, an initial assessment is carried out using pushover analysis to identify DS thresholds and then apply the CSM to evaluate the CDR_{LS} before any intervention through retrofitting.

Figure 4(a) shows the pushover curve with the horizontal axis representing the MIDR among all stories and the vertical axis showing the base shear. The first occurrence of some damage observations are also illustrated in Figure 4(a), such as first yield for beams and columns, SD for columns and joints (θ_{SD} and γ_{SD}), and joint failure (γ_u); mainly external ones. The MIDR thresholds for all DSs are also summarized in Table 3.

It can be observed in Figure 4(a) that both DS2 and DS3 are controlled by the limit states of the joints, which take place before those pertaining to the columns. It is also noticed that the beams do not reach their θ_{SD} and θ_u despite their yielding. This demonstrates that the nonlinear deformation is concentrated in the columns and joints, which depicts a non-ductile joint and column-sway mechanism. Accordingly, retrofitting efforts must be directed towards improving the key properties (i.e. strength, ductility, stiffness) of these structural components in particular, which will eventually improve the overall plastic mechanism of the building towards a beam-sway one (mainly characterized by beam hinging).

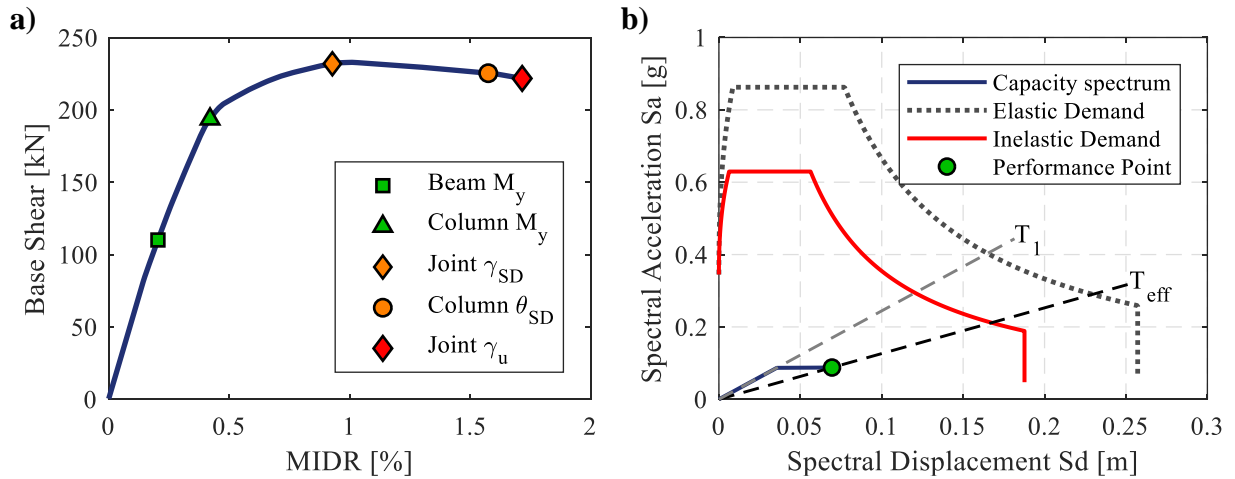


Figure 4: (a) Assessment for the as-built structure using pushover analysis and damage observations; (b) Graphical illustration for the capacity and demand spectra using the CSM

Damage state (DS)	DS1	DS2	DS3
MIDR threshold [%]	0.41	0.93	1.71

Table 3: MIDR thresholds for different DSs derived from pushover analysis

Figure 4(b) illustrates the idealized capacity spectrum of the equivalent SDoF system and the demand spectrum, both elastic and inelastic, plotted in the ADRS space. Applying the CSM, it is found that the inelastic demand spectrum significantly exceeds the capacity of the as-built structure. In other words, the performance point (PP) cannot intersect the inelastic demand spectrum, thus indicating a CDR_{LS} less than 1.0. According to Figure 4(b), the maximum capacity corresponds to a spectral displacement (Sd) of 0.07 m only. However, the expected demand displacement identified through the intersection between the secant stiffness line and the inelastic demand spectrum is nearly 0.167 m. Therefore, the CDR_{LS} of the as-built structure is very low, *i.e.* 42%, demonstrating the need for structural retrofitting.

3.2 Designed retrofitting solutions

As mentioned in section 2.3, the as-built structure is retrofitted with varying intervention levels to achieve the selected performance objectives (see Table 2). This process resulted in 13 retrofitted case studies using FRP wrapping of columns and joints, 15 cases for steel jacketing, and 18 for RC jacketing. The details, layout, and amount of retrofitted elements using FRP for all performance objective are listed in Table 4. For the sake of brevity, only one retrofitted case-study is described for each performance objective; particularly the one that satisfies the objective with the minimum possible amount of intervention.

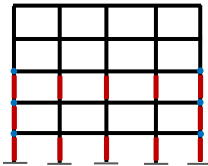
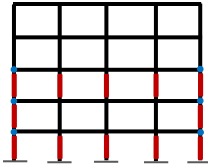
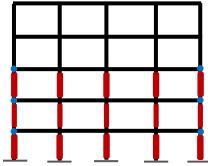
Performance objective	Achieved CDR_{LS}	Description of FRP retrofitting	Graphical illustration
No-collapse performance	65.4%	1 layer for external columns and joints in the 1 st to 3 rd floor and 1 layer for internal columns in the 1 st and 3 rd floors	
Limited performance	75.5%	Same joint retrofitting as above. 2 layers for the 3 rd floor columns and internal columns of the 1 st floor. 1 layer for external columns in 1 st to 2 nd floor.	
Basic performance	105.0%	Same joint retrofitting as above. 1 layer for the 2 nd floor columns. 4 layers for the 1 st floor and internal columns in 3 rd floor and 5 layers for the 3 rd floor external columns.	
Advanced performance	N.A.	N.A.	N.A.

Table 4: Description of FRP retrofitting alternatives for different performance objectives

Table 4 demonstrates that the advanced performance objective could not be achieved using FRP retrofitting. This is because FRP wrapping improves ductility through confinement and increases shear strength while its contribution to the lateral strength and stiffness is minimal (less than 10% in the current study). In fact, enhancing these parameters (*i.e.* stiffness and lateral strength) is essential with respect to moderate damage PL (or DS1) as the columns will not yield quickly, especially at low IM levels. It should be noted that the maximum value of CDR_{LS}

that could be achieved is around 110% since the number of FRP layers that could be applied for the columns cannot exceed five layers (see section 2.3).

Table 5 provides similar information about the retrofitted case studies using steel jacketing. It was possible to generate many cases of retrofitted buildings with large values of CDR_{LS} , particularly up to 147%. This is related to the high effectiveness of circular/elliptical jackets with respect to the high and continuous (radial) confinement they provide. This, in turn, significantly improves the ductility of the columns, thus making them capable of sustaining large levels of inelastic deformation. This also improved the (near) collapse situation, allowing beams to undergo failure prior to columns. Like the FRP case, all these advantages are insufficient to make the structure experience moderate damage (DS1) only against the LS demand (*i.e.* the advanced performance level) for the same reasons explained previously regarding the FRP.

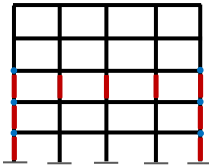
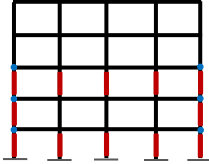
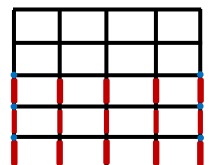
Performance objective	Achieved CDR_{LS}	Description of steel jacketing retrofitting	Graphical illustration
No-collapse performance	61%	1.5 mm thick jacket mm for the external columns in 1 st to 3 rd floor and internal ones in the 3 rd floor. Also retrofit external joints in 1 st to 3 rd floors using FRP.	
Limited performance	80%	Same joint retrofitting as above. Use 1.5 mm thick jacket for the external columns in the 1 st to 3 rd floor and internal ones in the 1 st and 3 rd floor	
Basic performance	106%	Same joint retrofitting as above. 1.5 mm thick jacket for the columns of 2 nd floor. 2.5 mm thick jackets for the 3 rd floor and external columns of 1 st floor. 3 mm jacket for the internal columns in 1 st floor	
Advanced performance	N.A.	N.A.	N.A.

Table 5: Description of steel jacketing retrofitting alternatives for different performance objectives

Finally, a summary for the case studies with RC jacketing is provided in Table 6, which shows that unlike FRP and steel jacketing, the advanced performance objective is achieved. This is because the RC jacketing provides a significant overall enhancement for the stiffness and strength, both shear and flexural, and improves the ductility through confinement. These features can also shift the building mechanism from local (*e.g.* soft-storey) to global, *i.e.* beam-sway. Therefore, the (frame-level) MIDR threshold of DS1 becomes much higher, and the retrofitted structure will not be easily subjected to yielding and moderate damages, especially at low IM levels. Nevertheless, as illustrated in Table 6, achieving the advanced performance level requires retrofitting the entire columns in the frame, thus making a global intervention to the frame rather than local, which might be expensive and technically challenging.

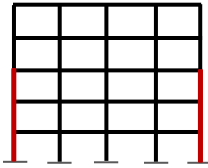
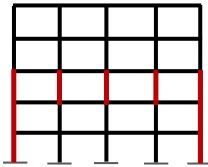
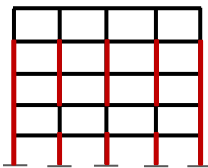
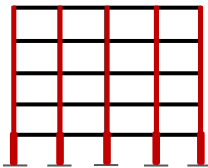
Performance objective	Achieved CDR_{LS}	Description of RC jacketing retrofitting	Graphical illustration
No-collapse performance	65%	Retrofit external columns in the 1 st to 3 rd floor with 50 mm jacket with 4 Φ 14 mm bars and 1 Φ 8/150 mm hoops.	
Limited performance	78%	50 mm jackets for the external columns in the 1 st to 3 rd floor with 4 Φ 14 mm bars and 1 Φ 8/150 mm hoops. 50 mm jackets for the internal columns of the 3 rd floor with 4 Φ 16 mm bars and 1 Φ 8/150 mm hoops	
Basic performance	105%	50 mm jackets for the external columns in the 1 st to 4 th floor with 4 Φ 14 mm bars and 1 Φ 8/150 mm hoops. 50 mm jackets for the internal columns in 1 st , 3 rd , 4 th floors with 4 Φ 16 mm bars and 1 Φ 8/150 mm hoops	
Advanced performance	181%	100 mm jackets with 8 Φ 16 mm bars and 1 Φ 8/100 mm hoops for external, and with 12 Φ 22 mm bars and 1 Φ 10/80 mm hoops for the internal columns of 1 st floor. 50 mm jackets with 8 Φ 20 mm bars and 1 Φ 8/150 mm hoops for external and with 8 Φ 22 mm bars and 1 Φ 8/150 for the internal columns of 2 nd floor. 50 mm jackets with 8 Φ 14 mm bars and 1 Φ 8/150 mm hoops for the 3 rd , 5 th and external columns of 4 th floor. Similar jackets but with 8 Φ 16 mm bars for internal columns of the 4 th floor	

Table 6: Description of RC jacketing retrofitting alternatives for different performance objectives

3.3 Fragility assessment

Upon developing all the case studies, including both the as-built and retrofitted structures, NLTHA is performed using the selected set of ground-motion records to assess the performance and derive the corresponding fragility relationships. Figure 5 shows both the IM vs. EDP cloud along with the fitted PSDM and the derived fragility relationships for the as-built structure. As demonstrated by Figure 5(a), the following points must be highlighted:

- The as-built structure remained undamaged only in 19.3% of the analysis cases.
- Moderate damage (DS1) was experienced by the frame in 23.3% of the cases.
- The frame was subjected to DS2 in a considerable portion of cases, particularly 21.3%.

- The near-collapse condition characterized by DS3 was experienced by the as-built frame in a significant number of analysis cases, which represents 36%.

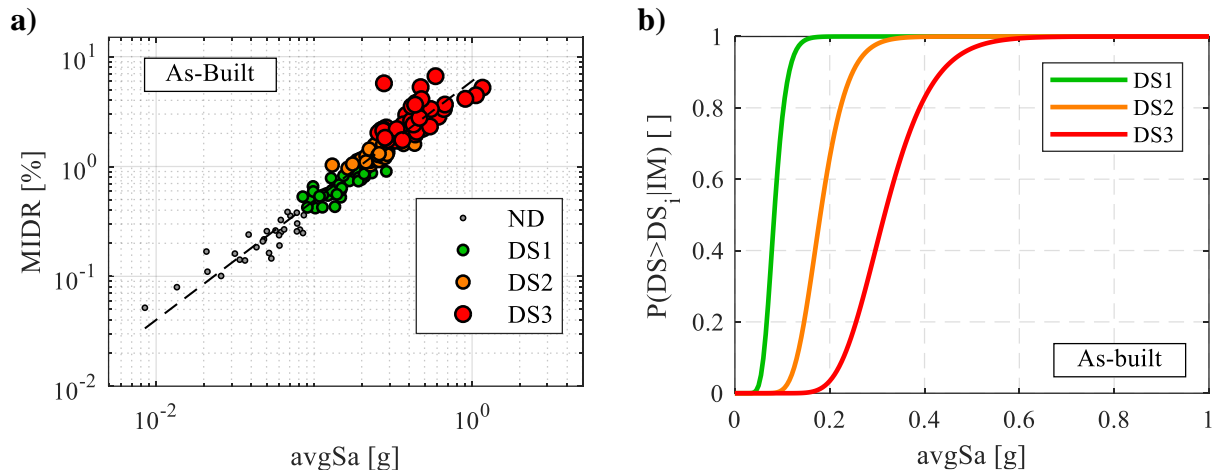


Figure 5: (a) IM vs EDP cloud; and (b) fragility relationships for the as-built structure

The poor performance of the as-built structure is reflected in the fragility relationships in Figure 5(b), which shows that the building is expected to experience high DSs, even at low IM levels. The fragility parameters including median (μ_{DS}) and dispersion (β) are given in Table 7.

DS	μ_{DS} [g]	β
DS1	0.083	
DS2	0.180	0.2504
DS3	0.316	

Table 7: Fragility parameters for the as-built structure

Fragility assessment is then carried out considering the retrofitted case studies defined previously. To illustrate the substantial impact of retrofitting, the fragility relationships for the as-built structure and the retrofitted cases are depicted in Figure 6. For each retrofitting technique, the fragility relationships for one retrofitted case only are plotted per performance objective, particularly the one that satisfied that objective with minimal intervention.

As per Figure 6, a significant improvement can be observed in the fragility relationships of DS2 and DS3 when the frames are retrofitted until satisfying the basic performance objective ($CDR_{LS} \approx 100\%$), which is represented by the rightward shift. This improvement is very similar for the three different retrofitting techniques but slightly higher for both steel and RC jacketing.

Figure 6(a),(b) demonstrate that the improvement in the fragility relationships of DS1, unlike DS2 and DS3, is relatively low when the frames are retrofitted using either FRP wrapping or steel jacketing. This can be explained by the fact that both techniques are mainly enhancing the ductility through confinement, in addition to prevention of shear failure, which is beneficial for DS2 and DS3 as they are associated with the performance of the building under high levels of inelastic deformation. On the other hand, improving DS1 fragility requires the enhancement of both lateral strength and stiffness to control the sway mechanism of the building and make it more difficult to develop moderate damages due to early yielding. However, the contribution of steel jacketing to the lateral strength and stiffness is minor compared to RC jacketing, whereas the contribution of FRP is approximately negligible.

In contrast, RC jacketing can change the mechanism of the building to a full beam-sway one. It also provides a significant overall improvement for all the aforementioned parameters, which resulted in a considerable shift in DS1 fragility relationship shown in Figure 6(c). Furthermore, the advanced performance objective could also be achieved using RC jacketing, which caused a considerable shift in the fragility relationships of the three DSs.

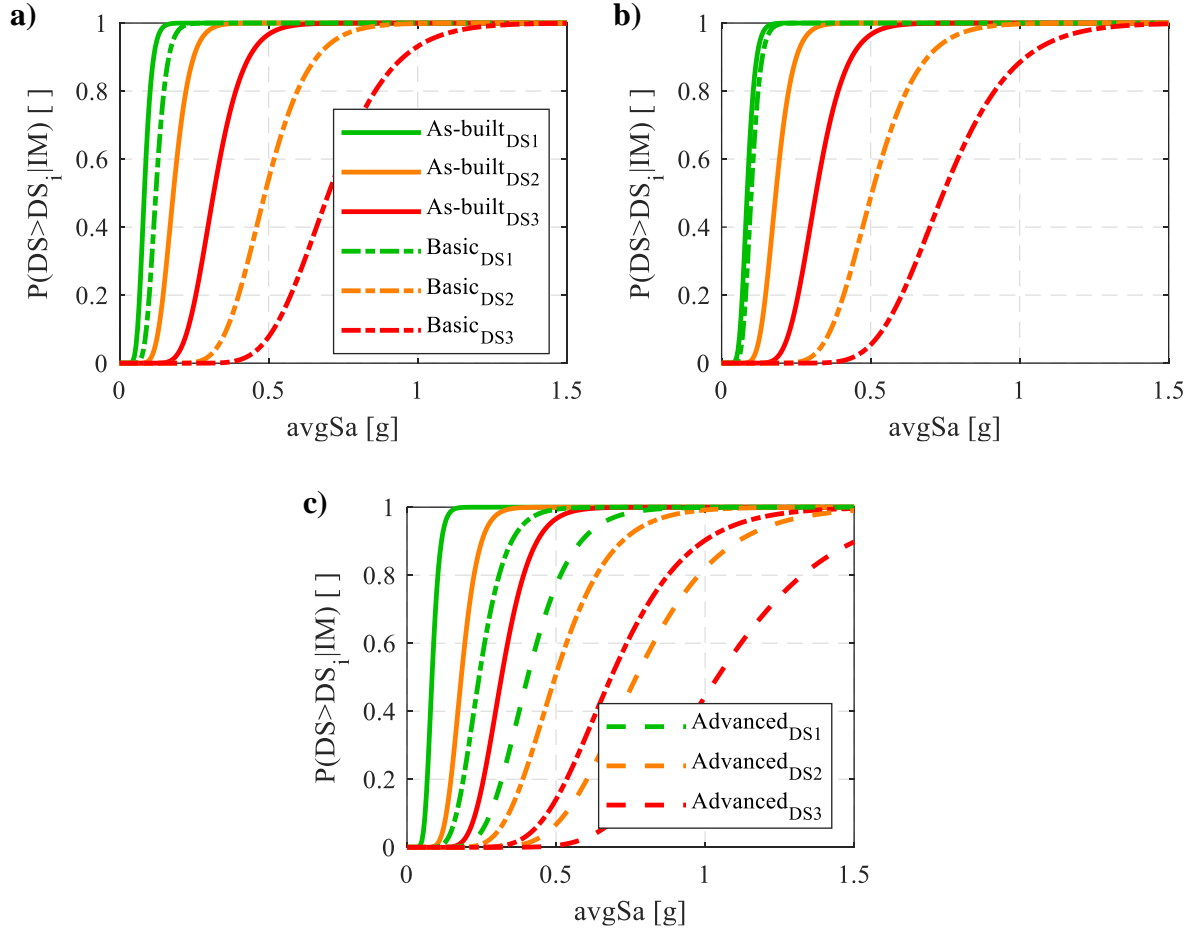


Figure 6: Fragility relationships for different performance objectives considering (a) FRP wrapping; (b) steel jacketing; and (c) RC jacketing

Overall, the previous analysis shows that the three techniques are similar with respect to improving the fragility relationships for the significant damage (DS2) and near collapse (DS3) conditions. In contrast, the improvement in DS1 fragility relationships is trivial if the FRP or steel jacketing are used. This indicates that structures retrofitted using these two techniques will remain highly susceptible to moderate damages, even at low ground-shaking levels.

4 CORRELATION BETWEEN CDR AND FRAGILITY PARAMETERS

The current study also attempts to map the improvement in the seismic performance of the case-study frame due to the varying retrofitting levels to the corresponding reduction in fragility. A reasonable approach to address this task is by correlating a simplified performance metric, which is the CDR_{LS} in this study, to the median of all fragility relationships, *i.e.* μ_{DS} . This is shown in Figure 7. A gradual increase in the values of μ_{DS} for DS2 and DS3 is observed for all the retrofitting techniques, which results from the performance improvement characterized by the CDR_{LS} . A sudden jump in the values of μ_{DS} can be also noticed in Figure 7(c) for the RC

jacketing, particularly at a CDR_{LS} close to 90%. This jump represents the case in which the RC jacketing becomes very effective due to the shift of the failure mechanism to beam sway.

In contrast, the overall increase in μ_{DS} of DS1 is trivial for both FRP wrapping and steel jacketing, as demonstrated by Figure 7(a),(b), even at very high levels of CDR_{LS} (see Section 3.3 for the discussion on this result). In fact, only the RC jacketing, with reference to Figure 7(c), is capable of significantly improving the μ_{DS} values for DS1, indicating that the structure becomes less susceptible to moderate damage, especially at low IM levels.

It should also be noticed that large values of CDR_{LS} could be reached using either steel or RC jacketing. After these levels, the retrofitting might become ineffective because the failure becomes associated with the beams rather than the columns and/or joints. However, the extent of CDR_{LS} increase in the case of the FRP technique is notably lower since a limited number of layers can be wrapped around to ensure confinement efficiency, as stated earlier.

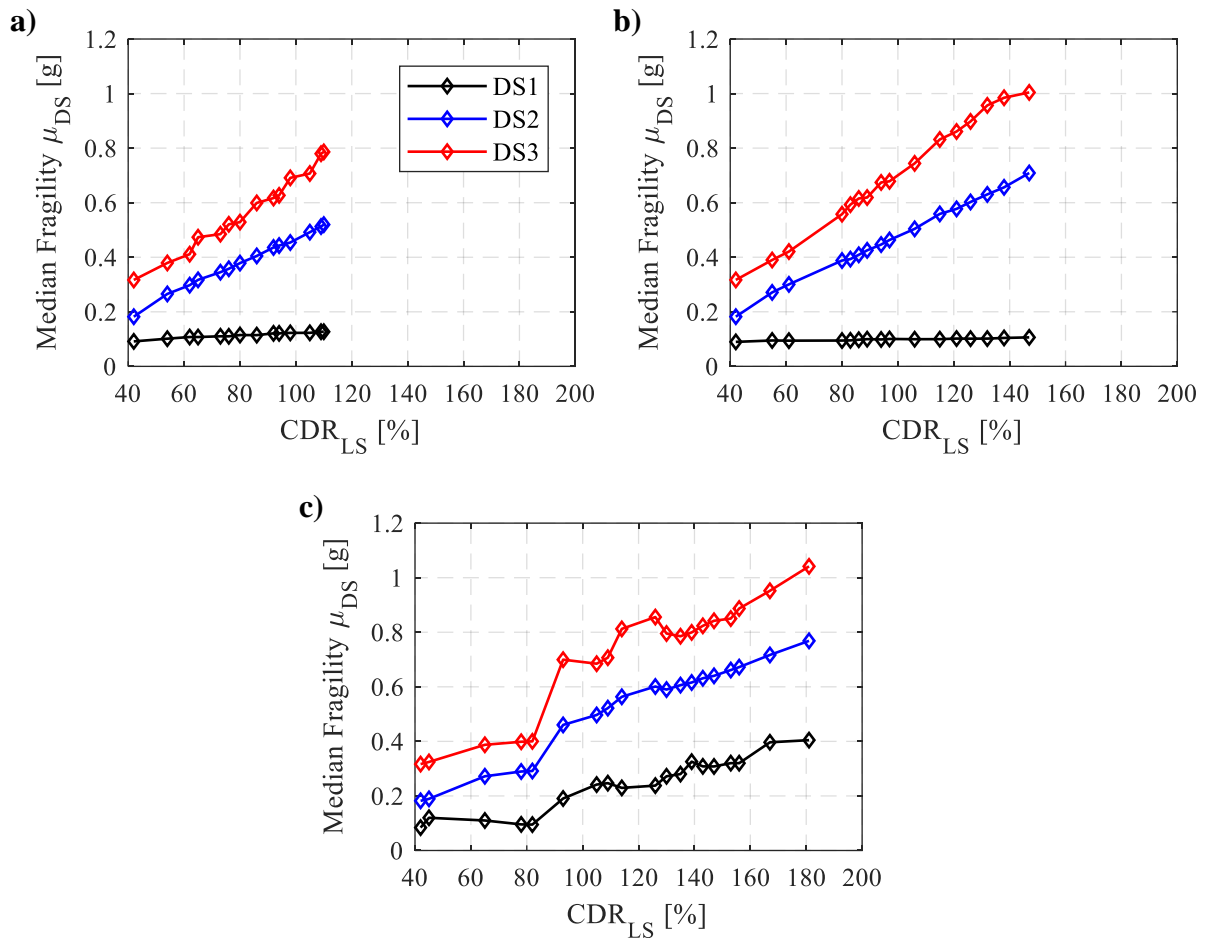


Figure 7: Variation of μ_{DS} against CDR_{LS} for (a) FRP wrapping; (b) steel jacketing; and (c) RC jacketing

A simplified model expressing the variation in μ_{DS} as a function of CDR_{LS} is defined by the best-fit line that minimizes the sum of squares of residuals (*i.e.* least-square approach). It should be noted that the variation of μ_{DS} is treated in a normalized fashion, which means that the developed expressions consider the variation in μ_{DS} resulting from retrofitting as a percentage of μ_{DS} of the as-built structure ($\Delta\mu_{DS}$). Figure 8 illustrates the fitted simplified models on the CDR_{LS} vs. $\Delta\mu_{DS}$ space, taking into account all the investigated DSs and retrofitting techniques. The coefficient of determination values (R^2) are also shown, which depict a clear linear trend between the two parameters. It must be noted that the initial CDR_{LS} is assumed equal to 42%.

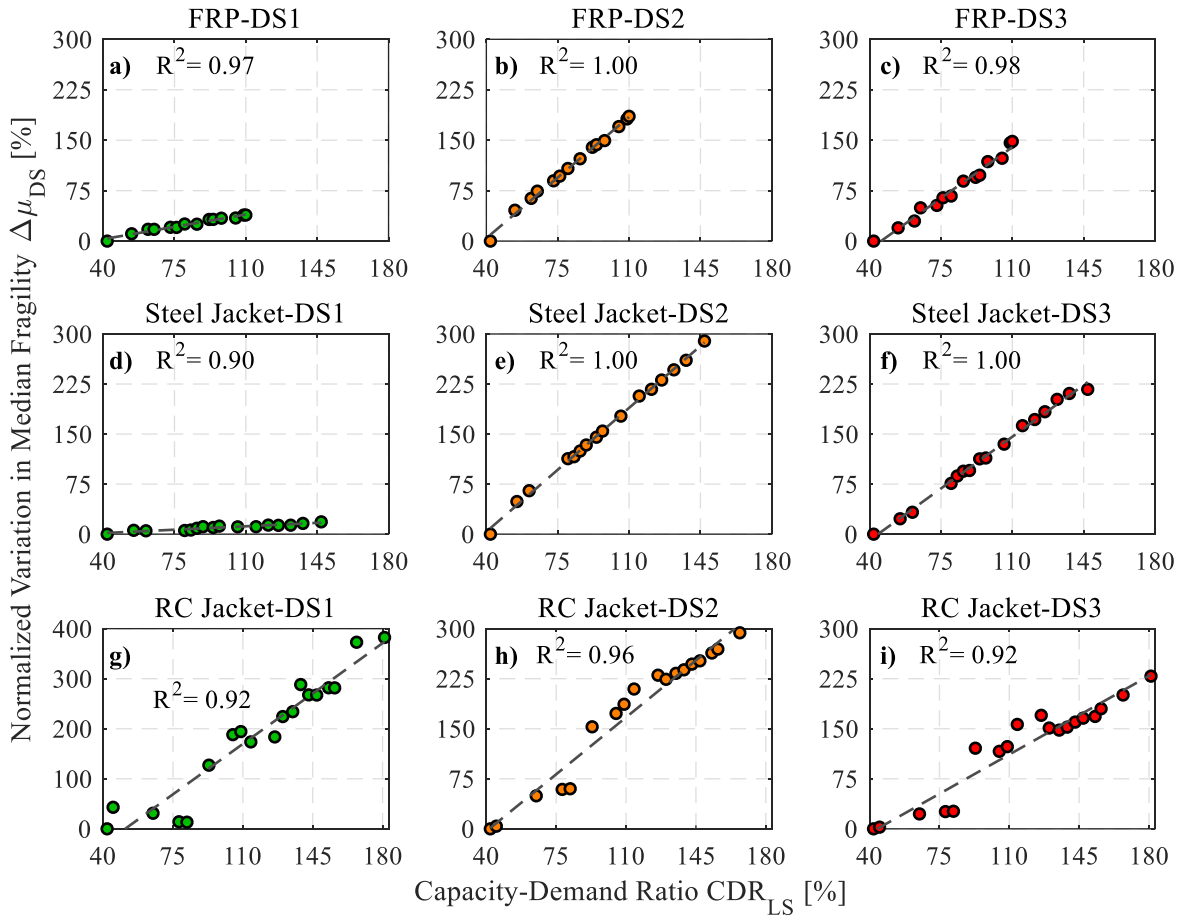


Figure 8: Correlation between the normalized variation of μ_{DS} against the CDR_{LS} for all DSs and techniques

The proposed simplified models can be easily used to provide reasonable estimates for the shift in fragility relationships of an as-built structure due to retrofitting once the CDR_{LS} is determined by just performing a pushover analysis. The outcome of these simplified models is directly used to modify the median values of the original fragility relationships to achieve the desired shift. Such an approach is deemed a quick and reasonable approximation in lieu of performing computationally expensive NLTHAs to derive new fragility relationships.

Nevertheless, it is important to highlight that the results obtained by the proposed models are limited by the uncertainties associated with the adopted modeling assumptions, material properties, geometry, layout, etc. Accordingly, additional research effort is needed to improve the accuracy of these expressions through incorporating additional case-study structures with different failure mechanisms, geometric/material properties, and layouts.

5 CONCLUSIONS

This study investigated the mapping between the improvement in seismic performance of a case-study RC frame and the seismic fragility reduction, which was achieved by designing and implementing varying structural retrofit levels. This is specifically characterized by correlating the increase in the CDR_{LS} values resulting from retrofitting to the shift of median parameters of fragility curves expressed by $\Delta\mu_{DS}$. The considered case study is an older non-ductile RC bare frame, which is designed to resist gravity loads only.

Three common and widely-used retrofitting techniques were adopted: FRP; steel jacketing, and RC jacketing. These techniques were designed via trial and error to achieve multiple

predefined performance objectives and thus generate numerous retrofitted case studies. The improvement in the seismic performance is initially quantified by applying pushover analysis in conjunction with the CSM in order to estimate CDR_{LS} for each case study.

The analysis of the as-built structure demonstrated a very poor seismic performance due to its susceptibility to high DSs, even at low IM levels. In contrast, a substantial improvement could be achieved through retrofitting. For example, fragility analysis showed that the μ_{DS} of DS2 and DS3 increased by at least 125% using any of the three techniques by just achieving the basic performance objective through retrofitting. However, only the RC jacketing was very effective in improving the DS1 fragility curves compared to FRP and steel jacketing. This is attributed to the fact that the latter two techniques improve ductility only, which is necessary for the DSs associated with high levels of nonlinear deformation, *i.e.* DS2 and DS3. Conversely, improving DS1 fragility curve requires enhancing both stiffness and lateral strength in addition to controlling lateral-sway mechanisms in order to make it difficult to develop early yielding and experience moderate damages, especially at low IM levels. This was possible to accomplish only by using the RC jacketing technique.

Finally, simple mathematical models were developed to relate the CDR_{LS} achieved by retrofitting to the $\Delta\mu_{DS}$ estimated using fragility analysis accounting for all DSs and retrofitting techniques. It is worth mentioning that these models are limited to the implemented case-study structure, modeling choices, and material properties. Therefore, additional research efforts are required in order to produce more generic models and reduce the uncertainty. After appropriate generalization, those expressions can be adopted to provide reasonable and quick quantification of the shift in median fragility parameters by just plugging in the value of CDR_{LS} , which can be calculated using simple pushover analyses. Such a simplified method can be used to analyze and/or design scenario-based retrofit implementation plans at a portfolio level, drastically reducing implementation efforts in a regional seismic risk model.

ACKNOWLEDGEMENTS

This study has received funding from project “Dipartimenti di Eccellenza”, funded by the Italian Ministry of Education, University and Research at IUSS Pavia. RG received additional funding from the European Union’s Horizon 2020 research and innovation programme under grant agreement No. 843794. (Marie Skłodowska-Curie Research Grants Scheme MSCA-IF-2018: MULTIRES, MULTI-level framework to enhance seismic RESilience of RC buildings).

REFERENCES

- [1] F. De Luca, G. E. D. Woods, C. Galasso, and D. D’Ayala, RC infilled building performance against the evidence of the 2016 EEFIT Central Italy post-earthquake reconnaissance mission: empirical fragilities and comparison with the FAST method, *Bulletin of Earthquake Engineering*, **16** (7), 2943–2969, 2018, doi: 10.1007/s10518-017-0289-1.
- [2] P. Ricci, F. de Luca, and G. M. Verderame, 6th April 2009 L’Aquila earthquake, Italy: Reinforced concrete building performance, *Bulletin of Earthquake Engineering*, **9**, 285–305, 2011, doi: 10.1007/s10518-010-9204-8.
- [3] J. P. Stewart *et al.*, Reconnaissance of 2016 central Italy earthquake sequence, *Earthquake Spectra*, **34** (4), 1547–1555, 2018, doi: 10.1193/080317EQS151M.
- [4] H. Kaplan, S. Yilmaz, N. Cetinkaya, and E. Atimtay, Seismic strengthening of RC structures with exterior shear walls, *Sadhana - Academy Proceedings in Engineering*

- Sciences*, **36** (1), 17–34, 2011, doi: 10.1007/s12046-011-0002-z.
- [5] A. Miano, H. Sezen, F. Jalayer, and A. Prota, Performance-based comparison of different retrofit methods for reinforced concrete structures, *COMPADYN 2017 - Proceedings of the 6th International Conference on Computational Methods in Structural Dynamics and Earthquake Engineering*, **1**, 1515–1535, 2017, doi: 10.7712/120117.5510.17150.
- [6] M. Badoux and J. O. Jirsa, Steel Bracing of RC Frames for Seismic Retrofitting, *Journal of Structural Engineering*, **116** (1), 55–74, 1990, doi: 10.1061/(asce)0733-9445(1990)116:1(55).
- [7] F. Freddi, E. Tubaldi, L. Ragni, and A. Dall’Asta, Probabilistic performance assessment of low-ductility reinforced concrete frames retrofitted with dissipative braces, *Earthquake Engineering and Structural Dynamics*, **42**, 993–1011, 2013, doi: 10.1002/eqe.2255.
- [8] A. Natale, C. Del Vecchio, and M. Di Ludovico, Seismic retrofit solutions using base isolation for existing RC buildings: economic feasibility and pay-back time, *Bulletin of Earthquake Engineering*, **19** (1), 483–512, 2021, doi: 10.1007/s10518-020-00988-9.
- [9] M. J. N. Priestley, F. Seible, Y. Xiao, and R. Verma, Steel jacket retrofitting of reinforced concrete bridge columns for enhanced shear strength. Part 2: Test results and comparison with theory, *ACI Materials Journal*, **91** (5), 537–551, 1994, doi: 10.14359/4168.
- [10] R. S. Aboutaha, M. U. Engelhardt, J. O. Jirsa, and M. F. Kreger, Retrofit of concrete columns with inadequate lap splices by the use of rectangular steel jackets, *Earthquake Spectra*, **12** (4), 693–714, 1996, doi: 10.1193/1.1585906.
- [11] R. S. Aboutaha, M. D. Engelhardt, J. O. Jirsa, and M. E. Kreger, Rehabilitation of shear critical concrete columns by use of rectangular steel jackets, *ACI Structural Journal*, **96** (1), 68–78, 1999, doi: 10.14359/597.
- [12] J. C. Alvarez, S. F. Breña, and S. R. Arwade, Nonlinear backbone modeling of concrete columns retrofitted with fiber-reinforced polymer or steel jackets, *ACI Structural Journal*, **115** (1), 53–64, 2018, doi: 10.14359/51700779.
- [13] M. J. N. Priestley and F. Seible, Design of seismic retrofit measures for concrete and masonry structures, *Construction and Building Materials*, **9** (6), 365–377, 1995, doi: 10.1016/0950-0618(95)00049-6.
- [14] F. Seible, M. J. N. Priestley, G. A. Hegemier, and D. Innamorato, Seismic Retrofit of RC Columns with Continuous Carbon Fiber Jackets, *Journal of Composites for Construction*, **1** (2), 52–62, 1997, doi: 10.1061/(asce)1090-0268(1997)1:2(52).
- [15] L. Lam and J. G. Teng, Design-oriented Stress – Strain Model for FRP-confined Concrete in Rectangular Columns, *Construction and Building Materials*, **17** (6–7), 471–489, 2003, doi: 10.1016/S0950-0618(03)00045-X.
- [16] M. J. N. Priestley, F. Seible, and G. M. Calvi, *Seismic Design and Retrofit of Bridges*. 1996.
- [17] M. Rodriguez and R. Park, Seismic load tests on reinforced concrete columns strengthened by jacketing, *ACI Structural Journal*, **91** (2), 150–159, 1994, doi: 10.14359/4593.
- [18] A. B. Liel and G. G. Deierlein, Cost-benefit evaluation of seismic risk mitigation alternatives for older concrete frame buildings, *Earthquake Spectra*, **29** (4), 1391–1411, 2013, doi: 10.1193/030911EQS040M.

- [19] D. Cardone, G. Gesualdi, and G. Perrone, Cost-Benefit Analysis of Alternative Retrofit Strategies for RC Frame Buildings, *Journal of Earthquake Engineering*, **23** (2), 208–241, 2019, doi: 10.1080/13632469.2017.1323041.
- [20] R. Gentile and C. Galasso, Simplified seismic loss assessment for optimal structural retrofit of RC buildings, *Earthquake Spectra*, **37** (1), 346–365, 2021, doi: 10.1177/8755293020952441.
- [21] V. Ligabue, S. Pampanin, and M. Savoia, Seismic performance of alternative risk-reduction retrofit strategies to support decision making, *Bulletin of Earthquake Engineering*, **16** (7), 3001–3030, 2018, doi: 10.1007/s10518-017-0291-7.
- [22] C. C. Harrington and A. B. Liel, Indicators of improvements in seismic performance possible through retrofit of reinforced concrete frame buildings, *Earthquake Spectra*, **37** (1), 262–283, 2021, doi: 10.1177/8755293020936707.
- [23] NZSEE, Assessment and improvement of the structural performance of buildings in earthquakes, 2006.
- [24] G. Calvi, G. Magenes, and S. Pampanin, Relevance of beam-column joint damage and collapse in rc frame assessment, *Journal of Earthquake Engineering*, **6** (1), 75–100, 2002, doi: 10.1080/13632460209350433.
- [25] G. M. Calvi, G. Magenes, and S. Pampanin, Experimental Test on a Three Storey RC Frame Designed for Gravity Only, in *Proceedings of the Twelfth European Conference on Earthquake Engineering*, 2002.
- [26] S. Pampanin, G. M. Calvi, and M. Moratti, Seismic behaviour of RC beam-column joints designed for gravity loads, in *12th European Conference on Earthquake Engineering*, 2002.
- [27] F. Braga, G. De Carlo, G. F. Corrado, R. Gigliotti, M. Laterza, and D. Nigro, Meccanismi di risposta di nodi trave-pilastro in ca di strutture non antisismiche, *X Congr. Naz. “L’ingegneria Sismica in Italia*, 9–13, 2001.
- [28] A. Masi, A. Digrisolo, and G. Santarsiero, Concrete strength variability in Italian RC buildings: Analysis of a large database of core tests, *Applied Mechanics and Materials*, **597**, 283–290, 2014, doi: 10.4028/www.scientific.net/AMM.597.283.
- [29] S. Caprili, L. Nardini, and W. Salvatore, Evaluation of seismic vulnerability of a complex RC existing building by linear and nonlinear modeling approaches, *Bulletin of Earthquake Engineering*, **10** (3), 913–954, 2012, doi: 10.1007/s10518-011-9329-4.
- [30] Verderame, A. Stella, and E. Cosenza, Le proprietà meccaniche degli acciai impiegati nelle strutture in c.a. realizzate negli anni ’60, *X Congresso Nazionale “L’Ingegneria Sismica in Italia” - ANIDIS*, 2001.
- [31] M. L. Puppio, M. Pellegrino, L. Giresini, and M. Sassu, Effect of material variability and mechanical eccentricity on the seismic vulnerability assessment of reinforced concrete buildings, *Buildings*, **7** (3), 15–17, 2017, doi: 10.3390/buildings7030066.
- [32] B. Lizundia, W. T. Holmes, K. Cobeen, J. Malley, and H. S. Lew, Techniques for the seismic rehabilitation of existing buildings, *8th US National Conference on Earthquake Engineering 2006*, **6**, 3646–3656, 2006.
- [33] ACI 440.2R, *Guide for the Design and Construction of Externally Bonded FRP Systems*. 2008.
- [34] P. E. Pinto, Istruzioni per la Valutazione Affidabilistica della Sicurezza Sismica di

- Edifici Esistenti CNR-DT 212/2013, *CNR – Commissione di studio per la predisposizione e l'analisi di norme tecniche relative alle costruzioni*, 190, 2014.
- [35] F. McKenna, OpenSees: A framework for earthquake engineering simulation, *Computing in Science and Engineering*, **13** (4), 58–66, 2011, doi: 10.1109/MCSE.2011.66.
- [36] M. J. N. Priestley, G. M. Calvi, and M. J. Kowalsky, *Displacement-Based Seismic Design of Structures*. Pavia: Fondazione EUCENTRE, IUSS Press, 2007.
- [37] M. M. Karthik and J. B. Mander, Stress-block parameters for unconfined and confined concrete based on a unified stress-strain model, *Journal of Structural Engineering*, **137** (2), 270–273, 2011, doi: 10.1061/(ASCE)ST.1943-541X.0000294.
- [38] G. J. O'Reilly and T. J. Sullivan, Modeling Techniques for the Seismic Assessment of the Existing Italian RC Frame Structures, *Journal of Earthquake Engineering*, **23** (8), 1262–1296, 2019, doi: 10.1080/13632469.2017.1360224.
- [39] H. Sezen and J. P. Moehle, Shear strength model for lightly reinforced concrete columns, *Journal of Structural Engineering*, **130** (11), 1692–1703, 2004, doi: 10.1061/(ASCE)0733-9445(2004)130:11(1692).
- [40] P. E. Mergos and A. J. Kappos, A gradual spread inelasticity model for R/C beam-columns, accounting for flexure, shear and anchorage slip, *Engineering Structures*, **44**, 94–106, 2012, doi: 10.1016/j.engstruct.2012.05.035.
- [41] D. K. Zimos, P. E. Mergos, and A. J. Kappos, Shear hysteresis model for reinforced concrete elements including the post-peak range, *COMPADYN 2015 - 5th ECCOMAS Thematic Conference on Computational Methods in Structural Dynamics and Earthquake Engineering*, (May), 2640–2658, 2015, doi: 10.7712/120115.3565.1184.
- [42] M. J. N. Priestley, *Displacement-based seismic assessment of reinforced concrete buildings*, **1** (1). 1997.
- [43] S. Pampanin, G. Magenes, and A. Carr, Modelling of shear hinge mechanism in poorly detailed RC beam-column joints, *Proceedings of the fib Symposium 2003: Concrete Structures in Seismic Regions*, (May 2014), 126–127, 2003.
- [44] J. B. Mander, M. J. Priestley, and R. Park, Theoretical stress-strain model for confined concrete, *Journal of Structural Engineering*, **114** (8), 1804–1826, 1988, doi: 10.1061/(ASCE)0733-9445(1988)114:8(1804).
- [45] C. C. Harrington and A. B. Liel, Evaluation of Seismic Performance of Reinforced Concrete Frame Buildings with Retrofitted Columns, *Journal of Structural Engineering*, **146** (11), 04020237, 2020, doi: 10.1061/(asce)st.1943-541x.0002801.
- [46] S. N. Bousias, D. Biskinis, M. N. Fardis, and A. L. Spathis, Strength, stiffness, and cyclic deformation capacity of concrete jacketed members, *ACI Structural Journal*, **104** (2), 521–531, 2007, doi: 10.14359/18854.
- [47] K. Aljawhari, R. Gentile, F. Freddi, and C. Galasso, Effects of ground-motion sequences on fragility and vulnerability of case-study reinforced concrete frames, *Bulletin of Earthquake Engineering*, 2020, doi: 10.1007/s10518-020-01006-8.
- [48] EN 1998-3, Eurocode 8: Design of structures for earthquake resistance – Part 3: Assessment and retrofitting of buildings [Authority: The European Union Per Regulation 305/2011, Directive 98/34/EC, Directive 2004/18/EC], Brussels, 2005.
- [49] K. Aljawhari, F. Freddi, and C. Galasso, State-dependent vulnerability of case-study

- reinforced concrete frames, in *7th International Conference on Computational Methods in Structural Dynamics and Earthquake Engineering, COMPDYN 2019; Crete, Greece; June 24-26, 2019*.
- [50] ASCE/SEI 41-13, American Society of Civil Engineers ASCE standard ASCE/SEI 41-13: seismic evaluation and retrofit of existing buildings, American Society of Civil Engineers, Reston, Virginia, 2013.
- [51] FEMA, Prestandard and Commentary for the Seismic Rehabilitation of Buildings, *Rehabilitation Requirements*, (1), 1–518, 2000.
- [52] A. Atc, 40, Seismic evaluation and retrofit of concrete buildings, *Applied Technology Council*, **1**, 334, 1996.
- [53] EN 1998-1, Eurocode 8: Design of structures for earthquake resistance - Part 1 : General rules, seismic actions and rules for buildings [Authority: The European Union Per Regulation 305/2011, Directive 98/34/EC, Directive 2004/18/EC], Brussels, 2004.
- [54] F. Jalayer, R. De Risi, and G. Manfredi, Bayesian Cloud Analysis: Efficient structural fragility assessment using linear regression, *Bulletin of Earthquake Engineering*, **13**, 1183–1203, 2015, doi: 10.1007/s10518-014-9692-z.
- [55] C. A. Cornell, F. Jalayer, R. O. Hamburger, and D. A. Foutch, Probabilistic Basis for 2000 SAC Federal Emergency Management Agency Steel Moment Frame Guidelines, *Journal of Structural Engineering*, **128** (4), 526–533, 2002, doi: 10.1061/(asce)0733-9445(2002)128:4(526).
- [56] C. Smerzini, C. Galasso, I. Iervolino, and R. Paolucci, Ground motion record selection based on broadband spectral compatibility, *Earthquake Spectra*, **30** (4), 1427–1448, 2014, doi: 10.1193/052312EQS197M.
- [57] R. Gentile, C. Galasso, Y. Idris, I. Rusydy, and E. Meilianda, From rapid visual survey to multi-hazard risk prioritisation and numerical fragility of school buildings, *Natural Hazards and Earth System Sciences*, **19** (7), 1365–1386, 2019, doi: 10.5194/nhess-19-1365-2019.
- [58] J. W. Baker and C. A. Cornell, Spectral shape, epsilon and record selection, *Earthquake Engineering and Structural Dynamics*, **35** (9), 1077–1095, 2006, doi: 10.1002/eqe.571.
- [59] A. K. Kazantzi and D. Vamvatsikos, Intensity measure selection for vulnerability studies of building classes, *Earthquake Engineering and Structural Dynamics*, **44** (15), 2677–2694, 2015, doi: 10.1002/eqe.2603.
- [60] M. Kohrangi, P. Bazzurro, D. Vamvatsikos, and A. Spillatura, Conditional spectrum-based ground motion record selection using average spectral acceleration, *Earthquake Engineering and Structural Dynamics*, **46** (10), 1667–1685, 2017, doi: 10.1002/eqe.2876.
- [61] S. Minas and C. Galasso, Accounting for spectral shape in simplified fragility analysis of case-study reinforced concrete frames, *Soil Dynamics and Earthquake Engineering*, **119** (August 2018), 91–103, 2019, doi: 10.1016/j.soildyn.2018.12.025.
- [62] M. Kohrangi, P. Bazzurro, and D. Vamvatsikos, Vector and scalar IMs in structural response estimation, Part II: Building demand assessment, *Earthquake Spectra*, **32** (3), 1525–1543, 2016, doi: 10.1193/053115EQS081M.